



L-Arginine increases AMPK phosphorylation and the oxidation of energy substrates in hepatocytes, skeletal muscle cells, and adipocytes

Wenjuan S. Jobgen¹ · Guoyao Wu¹

Received: 27 March 2022 / Accepted: 1 August 2022 / Published online: 16 August 2022
© The Author(s), under exclusive licence to Springer-Verlag GmbH Austria, part of Springer Nature 2022

Abstract

Previous work has shown that dietary L-arginine (Arg) supplementation reduced white fat mass in obese rats. The present study was conducted with cell models to define direct effects of Arg on energy-substrate oxidation in hepatocytes, skeletal muscle cells, and adipocytes. BNL CL.2 mouse hepatocytes, C2C12 mouse myotubes, and 3T3-L1 mouse adipocytes were treated with different extracellular concentrations of Arg (0, 15, 50, 100 and 400 μM) or 400 μM Arg + 0.5 mM *N*^G-nitro-L-arginine methyl ester (L-NAME; an NOS inhibitor) for 48 h. Increasing Arg concentrations in culture medium dose-dependently enhanced ($P < 0.05$) the oxidation of glucose and oleic acid to CO_2 in all three cell types, lactate release from C2C12 cells, and the incorporation of oleic acid into esterified lipids in BNL CL.2 and 3T3-L1 cells. Arg at 400 μM also stimulated ($P < 0.05$) the phosphorylation of AMP-activated protein kinase (AMPK) in all three cell types and increased ($P < 0.05$) NO production in C2C12 and BNL CL.2 cells. The inhibition of NOS by L-NAME moderately reduced ($P < 0.05$) glucose and oleic acid oxidation, lactate release, and the phosphorylation of AMPK and acetyl-CoA carboxylase (ACC) in BNL CL.2 cells, but had no effect ($P > 0.05$) on these variables in C2C12 or 3T3-L1 cells. Collectively, these results indicate that Arg increased AMPK activity and energy-substrate oxidation in BNL CL.2, C2C12, and 3T3-L1 cells through both NO-dependent and NO-independent mechanisms.

Keywords Arginine · Metabolism · Muscle cells · Nitric oxide · Substrate oxidation · White adipocytes

Abbreviations

ACC	Acetyl-CoA carboxylase
AMPK	AMP-activated protein kinase
AU	Arbitrary unit
CPT-I	Carnitine palmitoyltransferase I
GAPDH	Glyceraldehyde-3-phosphate dehydrogenase
KHB	Krebs–Henseleit bicarbonate
MCD	Malonyl-CoA decarboxylase
L-NAME	<i>N</i> ^G -Nitro-L-arginine methyl ester
NO	Nitric oxide
NOS	Nitric oxide synthase
SCD-1	Stearoyl-CoA desaturase 1
SDS	Sodium dodecyl sulfate

S6K1	Ribosomal protein S6 kinase beta-1
TTBS	Tris–Tween-buffered saline

Introduction

Nitric oxide (NO) is a free radical produced from L-arginine (Arg) by NO synthases (NOS) (Förstermann and Sessa 2012). Three isoforms of the NOS are expressed in various tissues, including insulin-sensitive tissues (liver, muscle and adipose tissue) that play an important role in whole-body homeostasis of energy substrates (Alderton et al. 2001; Förstermann et al. 1994; Jobgen et al. 2006). Besides endothelial cells (Raman et al. 1998), macrophages (Kröncke et al. 1991), and neurons (Schuman and Madison 1991), NO production has been detected for many other cell types, including hepatocytes (Nicholls-Grzemeski et al. 1999), skeletal muscle cells (Williams et al. 1994), and white adipocytes (Yan et al. 2002) under both basal and stimulated conditions. The actions of NO are mediated primarily by the activation of guanylyl cyclase and the resultant production of

Handling editor: E. Ildicho Closs.

✉ Guoyao Wu
g-wu@tamu.edu

¹ Department of Animal Science and Faculty of Nutrition, Texas A&M University, College Station, TX 77843, USA

guanosine 3',5'-cyclic monophosphate (cGMP) (Denninger and Marletta 1999).

Our previous studies using Zucker diabetic fatty rats (Fu et al. 2005) and diet-induced obese rats (Jobgen 2007; Jobgen et al. 2009) demonstrated that dietary supplementation with Arg increased glucose and fatty acid oxidation in skeletal muscle and white adipose tissue, therefore reducing body white-fat mass. Beneficial effects of Arg supplementation on reducing white fat, increasing lean tissue mass, and improving metabolic profiles have also been reported by many research groups for rodents and other members of the animal kingdom, including diet-induced obese rats (Alam et al. 2013; Miczke et al. 2015), mice (Sellmann et al. 2017), and sheep (Satterfield et al. 2012); growing-finishing pigs (Tan et al. 2011), poultry (Fouad et al. 2013), and fish (Li et al. 2020); individuals with diabetes mellitus (Mariotti 2020; Szlas et al. 2022); and obese persons (Boon et al. 2019; Khosroshahi et al. 2020; McNeal et al. 2018). Further, we found that the beneficial effect of Arg on metabolic health was mediated partially through the activation of hepatic AMP-activated protein kinase (AMPK) (Jobgen 2007; Jobgen and Wu 2022). However, the underlying biochemical mechanisms remain largely unknown (McKnight et al. 2010; Mariotti 2020; Szlas et al. 2022).

There is growing evidence that NO regulates energy metabolism in cells and animals (Dai et al. 2013; Durante 2020; Jobgen et al. 2006; Sansbury and Hill 2014; San Martín et al. 2017). Therefore, we hypothesized that Arg increased energy metabolism through enhancing NO production and activating AMPK. This hypothesis was tested using established cell models for hepatocytes, skeletal muscle cells and adipocytes (Chen et al. 2018; Lee et al. 1997; Wang and Watford 2007).

Materials and methods

Materials

BNL CL.2 mouse hepatocytes, C2C12 mouse skeletal muscle cells and 3T3-L1 mouse preadipocytes were obtained from ATCC (Manassa, VA). Arg-free customized Dulbecco's modified Eagle medium (DMEM) with 5 mM glucose and concentrations of other amino acids found in the plasma of adult rats (Jobgen et al. 2009), nutrient-rich DMEM, horse serum, trypsin-EDTA solution, penicillin (10,000 U/mL), streptomycin (10,000 µg/mL), and 4–12% NuPAGE Bis-Tris gels were purchased from Invitrogen (Grand Island, NY). Fetal bovine serum (FBS), NCS-II, and the bicinchoninic acid kit were procured from Hyclone (Logan, UT), Amer-sham (Piscataway, NJ), and Pierce (Rockford, IL), respectively. HPLC-grade methanol and water were purchased

from Fisher Scientific (Houston, TX). D-[U-¹⁴C]glucose and [1-¹⁴C]oleic acid were products of American Radiolabeled Chemicals (St Louis, MO). Protease inhibitor and phosphatase inhibitor cocktails were obtained from Calbiochem (La Jolla, CA). Unless indicated, all other chemicals were procured from Sigma-Aldrich (St Louis, MO).

Cell culture

BNL CL.2 cells, C2C12 cells, and 3T3-L1 cells were cultured in 100-mm dishes with 20 ml of nutrient-rich DMEM containing 10% FBS and 100 U/mL penicillin plus 100 µg/mL streptomycin until 75–80% confluent. Cells were trypsinized and split into 25-cm² Falcon flasks with approximately 2×10^5 cells per flask (10 ml medium) and maintained at 37 °C in a 5% CO₂ incubator. The basal nutrient-rich DMEM for cell culture contained 25 mM glucose, 4 mM glutamine, and 0.4 mM Arg. For our experiments, BNL CL.2 cells at confluence were used directly, whereas differentiated C2C12 and 3T3-L1 cells were employed. After C2C12 cells reached confluence, differentiation was initiated by substituting 10% FBS with 2% horse serum in the culture medium. The medium was changed every 2 days. Four days after the initiation of differentiation, myotubes were formed and then used for the experiment.

For differentiating 3T3-L1 cells, they were cultured in 20 ml of nutrient-rich DMEM with 10% FBS until confluence. Two days post-confluence, differentiation was initiated by switching the cells to nutrient-rich DMEM containing 10% FBS, 10 µg/mL insulin, 0.5 mM 3-isobutyl-1-methylxanthine, and 10 µM dexamethasone. Two days later, the medium was changed to nutrient-rich DMEM containing 10% FBS and 10 µg/mL insulin. After an additional 2 days, cells were switched to nutrient-rich DMEM containing 10% FBS. The medium was then changed every other day. Eight days after the initiation of cell differentiation, mature white adipocytes were obtained and then used for the experiment.

The day before performing an experiment, 3T3-L1 adipocytes and BNL CL.2 hepatocytes in 25-cm² Falcon flasks were switched to 10 ml of nutrient-rich DMEM containing 0.5% FBS for overnight, whereas C2C12 cells in 25-cm² Falcon flasks were maintained in 10 ml of nutrient-rich DMEM containing 2% horse serum. The concentrations of serum were chosen on the basis of the consideration that a high level might mask the effect of Arg, while cell viability might be compromised in serum-free medium. On the day of the experiment, all the three types of cells were switched to 10 ml of Arg-free customized DMEM containing 5 mM D-glucose, 0.5 mM L-glutamine, and 0.5% FBS; and this basal culture medium contained 0.7 µM Arg. Arg was then added to the medium,

providing concentrations of 0, 15, 50, 100, or 400 μM . In some experiments, culture medium contained 400 μM Arg plus 500 μM N^G -nitro-L-arginine methyl ester (L-NAME, an NOS inhibitor). To ensure optimal inhibition of NO production in cells, L-NAME was added to the medium 1 h earlier than Arg. All the cells were cultured at 37 °C for 48 h, with the medium being changed every 24 h. At the end of the 48-h culture period, cells were used for biochemical studies and the media were analyzed for nitrite (an indicator of NO synthesis) and amino acids (Jobgen et al. 2009). We determined that at the end of the last 24-h culture in the 10 ml fresh medium with initial concentrations of 0, 15, 50, 100, and 400 μM Arg, the concentrations of Arg in the conditioned medium (means \pm SEM, $n=4$) for C2C12 cells were 0.53 ± 0.05 , 8.5 ± 0.8 , 39 ± 2.5 , 83 ± 4.0 , and 356 ± 9.7 μM , respectively; the concentrations of Arg in the conditioned medium for BNL CL.2 cells were 0.51 ± 0.04 , 7.9 ± 0.6 , 35 ± 3.1 , 78 ± 4.6 , and 334 ± 9.2 μM , respectively; the concentrations of Arg in the conditioned medium for 3T3-L1 mouse adipocytes were 0.54 ± 0.04 , 8.2 ± 0.9 , 37 ± 3.6 , 80 ± 3.7 , and 342 ± 10 μM , respectively.

Glucose and oleic acid oxidation

Cells obtained through the above culture were rinsed with phosphate-buffered saline (PBS) three times, and were then incubated in the same 25-cm² Falcon flasks (placed within an unshaken cell culture incubator) at 37 °C in 2 mL of oxygenated (95% O₂/5% CO₂) Krebs–Henseleit bicarbonate buffer (KHB, pH 7.4) containing 5 mM D-glucose and either 0.5 μCi D-[U-¹⁴C]glucose or 0.2 mM oleic acid plus 0.5 μCi [1-¹⁴C]oleic acid. Arg or L-NAME was added to incubation medium to obtain the same respective concentrations as in the previous 48-h culture medium. The flasks were sealed tightly with rubber stoppers fitted with hanging center-wells, as we did in our previous studies of substrate oxidation by mammalian cells incubated in 25-ml polypropylene conical flasks (Wu et al. 1995). At the end of a 2-h incubation period, flasks were placed in the straight-up position, and 0.2 mL NCS-II (an alkaline solution to trap ¹⁴CO₂) was added through the stopper into a 500- μl microcentrifuge tube placed in the center-well, followed by the addition of 0.2 mL of 1.5 M HClO₄ to the incubation medium. Such a position of the flasks was adopted to prevent the drop of NCS-II to the incubation medium. After an additional 1-h incubation, the microcentrifuge tubes with NCS-II were carefully transferred to scintillation vials. Fifteen milliliters of counting cocktail (He and Wu 2022) were added to the vials and ¹⁴C radioactivity was determined by a Packard liquid scintillation counter (Wu et al. 1995). The specific

activities of D-[U-¹⁴C]glucose and [1-¹⁴C]oleic acid in the incubation media were used to calculate the rate of CO₂ production from glucose and oleic acid, respectively. The acid-lysed cell solution was centrifuged at 600 g for 10 min. The supernatant fluid was analyzed for lactate using an enzymatic method (Wu et al. 1995). The pellet fraction (protein) was washed three times with 5 ml of 2% trichloroacetic acid through centrifugation (600 g, 10 min), and then solubilized in 0.5 ml of 1 M NaOH (Wu and Thompson 1990) before the determination of protein concentration using the bicinchoninic acid kit.

Incorporation of glucose into lipids and of oleic acid into esterified lipids

The determination of D-[U-¹⁴C]glucose incorporated into lipids was performed as described by Ceddia et al. (2000). Briefly, the acidified incubation medium from the glucose oxidation experiment above was collected and mixed with 5 mL of Doles's reagent (isopropanol/*n*-heptane/H₂SO₄; 4:1:0.25, v/v/v; Dole and Meinertz 1960). The heptane layer, which contained lipids, was carefully transferred to scintillation counting vials and dried under a fumehood. Then, 15 mL of counting cocktail (Hionic Fluor, Packard, Meriden, CT) was added to the vials for the measurement of ¹⁴C radioactivity.

The incorporation of [1-¹⁴C]oleic acid into esterified lipids was determined as described by Oliveira and Vaughan (1964) with modifications. Briefly, the acidified incubation medium from the oleic acid oxidation experiment above was mixed with 15 mL of a chloroform–methanol solution (2:1, v/v). After shaking for 20 min, 9 mL of 4% Na₂CO₃ (w/v in water) was added, followed by 20 min of mixing. The tubes were then centrifuged to allow the separation of aqueous and chloroform layers. The chloroform layer was transferred into clean tubes and subjected to two more washes with 4% Na₂CO₃. After the chloroform layer [containing esterified lipids (triglycerides and other glycerol-based esters) but no oleic acid] was transferred to a scintillation vial and dried under a fumehood, 15 mL of counting cocktail (Hionic Fluor) was added to the vials for the measurement of ¹⁴C radioactivity.

Nitrite analysis

Nitrite in cell culture medium was analyzed using an HPLC method as described by Li et al. (2000). This technique offers the advantages of high sensitivity and specificity for the determination of nitrite as an oxidation product of nitric oxide (Jobgen et al. 2007). The medium without cells was included as blanks.

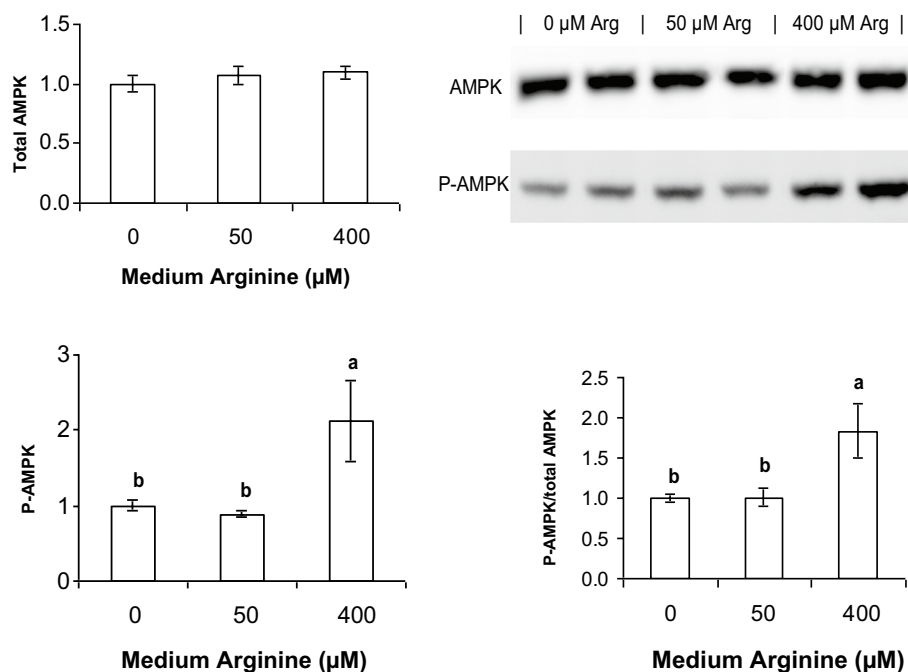


Fig. 1 Relative protein levels for total AMPK α , phosphorylated AMPK α (P-AMPK α) and the ratio of P-AMPK α to total AMPK α in BNL CL2 hepatocytes. Cells were cultured for 48 h in customized DMEM containing 0, 50 or 400 μ M L-arginine. The same amount of cell proteins (30 μ g) from different treatment groups was loaded into 4–12% SDS–polyacrylamide gels for the separation of

AMPK α and phosphorylated AMPK α proteins. The protein images were developed with the use of the Supersignal West Dura Extended Duration Substrate, and two representative blots from each treatment group are shown. Data, expressed as relative values to the cells cultured without added L-arginine, are means \pm SEM, $n=4$. Means with different letters are different ($P < 0.05$)

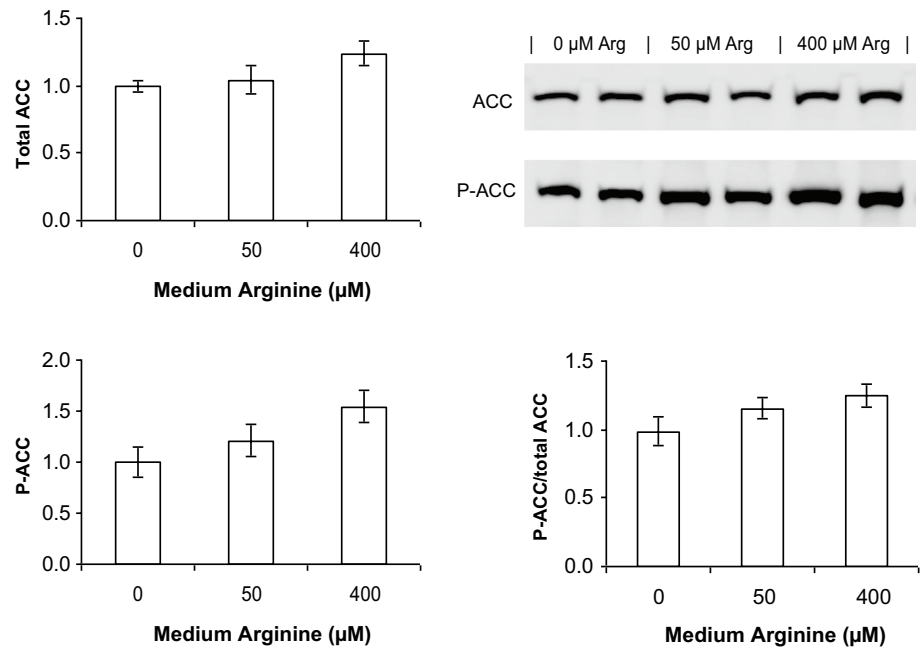
Western blot analysis

BNL CL2 cells, C2C12 cells, and 3T3-L1 cells were cultured for 48 h in the presence of 0, 50, 400 μ M Arg, or 400 μ M Arg plus 500 μ M L-NAME, as described above. After the 48-h culture period, cells were washed with PBS three times, followed by lysis in a buffer containing 20 mM Tris–HCl (pH 7.4), 50 mM NaCl, 50 mM NaF, 50 mM EDTA, 1% Triton X-100, 1 \times protease inhibitor cocktail, and 1 \times phosphatase inhibitor cocktail. Cells were then scraped off into tubes and centrifuged for 10 min at 10,000g. Protein content in the supernatant fraction was analyzed using the bicinchoninic acid kit. For western blot analysis, 30 μ g of protein in a sample was separated on 4–12% polyacrylamide gradient gels, transferred to nitrocellulose membranes, blocked with 5% fat-free dry milk in TTBS, and incubated with the following primary antibodies overnight at 4 $^{\circ}$ C with gentle rocking: AMPK α (Cat. #2532, Cell Signaling, 1:1000); phosphorylated AMPK α (Thr¹⁷²) (Cat. #2531, Cell Signaling, 1:1000); ACC (Cat. #3662, Cell Signaling, 1:1000, detecting all isoforms of ACC protein); and phosphorylated ACC (Ser⁷⁹) (Cat. #3661, Cell Signaling, 1:1000, recognizing both ACC1 and ACC2 proteins). After being washing three times with TTBS,

the membranes were incubated at 25 $^{\circ}$ C for 3 h with secondary antibodies at 1:50,000 (peroxidase-labeled donkey anti-goat or anti-rabbit IgG, Jackson Immuno Research). Finally, the membranes were washed with TTBS, followed by development using Supersignal West Dura Extended Duration Substrate according to the manufacturer's instructions (Pierce, Rockford, IL). The signals were detected on Fujifilm LAS-3000 (Tokyo, Japan).

After the last immunodetection, membrane-bound proteins were stained with Coomassie Blue R250 (ImperialTM Protein Stain; Pierce, Rockford, IL, USA) according to the manufacturer's instructions to verify the equal loading/transfer of tissue proteins. Briefly, the blotting membrane was washed for 2 min twice with deionized water and then stained with 0.1% Coomassie R-250 (Pierce) for 5 min. The stained membrane was washed 3 times with a solution of 50% methanol/10% acetic acid and then rinsed with 10% methanol. The dry membrane was scanned using Typhoon (Amersham Bioscience, Piscataway NJ, USA) and the staining density for all proteins in each complete lane was analyzed in the DeCyder software 6.5 (Amersham Bioscience), with the area outside the protein lanes being the background, as we described previously (Wang et al. 2008).

Fig. 2 Relative protein levels for total ACC, phosphorylated ACC (P-ACC) and the ratio of P-ACC to total ACC in BNL CL.2 hepatocytes. Cells were cultured for 48 h in customized DMEM containing 0, 50 or 400 μM L-arginine. The same amount of cell proteins (30 μg) from different treatment groups was loaded into 4–12% SDS–polyacrylamide gels for the separation of ACC and phosphorylated ACC proteins. The protein images were developed with the use of the Supersignal West Dura Extended Duration Substrate, and two representative blots from each treatment group are shown. Data, expressed as relative values to the cells cultured without added L-arginine, are means \pm SEM, $n=4$



Data expression and statistical analysis

In the western blotting, 4 samples (cell lysates) from each of the three treatment groups in Figs. 1, 2, 3, 4, 5 and 6 and from each of the two treatment groups in Figs. 7, 8 and 9 were loaded onto the same gel and the proteins were transferred to the same blotting membrane. Thus, the mean value in the bar graph represents the 4 samples per treatment group. Data, expressed as means \pm SEM, were analyzed using one-way ANOVA (Assaad et al. 2014). The Tukey multiple comparison method was used to determine differences among the means of the treatment groups for 0–400 μM Arg. The paired t test was employed to analyze the data for cells treated with either 400 μM Arg or 400 μM Arg plus 0.5 mM L-NAME. Probability values ≤ 0.05 were taken to indicate statistical significance.

Results

BNL CL.2 hepatocytes

Table 1 summarizes data on glucose and oleic acid oxidation, lactate production, and the incorporation of glucose into lipids and of oleic acid into esterified lipids in BNL CL.2 cells. There were no differences in glucose oxidation, oleic acid oxidation, or the incorporation of oleic acid into esterified lipids between 0 and 50 μM Arg. However, increasing medium concentrations of Arg from 50 to 400 μM increased ($P < 0.05$) glucose and oleic acid oxidation, as well as the incorporation of oleic acid into esterified lipids. Exposure of the cells up to 400 μM Arg had no effect on lactate

production or the incorporation of glucose into lipids. In the presence of various concentrations of Arg, a large amount of lactate was produced from glucose relative to the oxidation of glucose to CO_2 , whereas 85–90% of metabolized oleic acid was incorporated into esterified lipids in BNL CL.2 cells.

Staining intensities of total proteins bound to the blotting membrane for BNL CL.2 cells cultured with 0, 50, and 400 μM Arg were 1.000 ± 0.026 , 1.030 ± 0.038 , and 1.018 ± 0.025 AU, respectively ($P > 0.05$). Total and phosphorylated levels of AMPK and ACC in BNL CL.2 cells are presented in Figs. 1 and 2, respectively. There were no differences in total or phosphorylated AMPK or ACC between 0 and 50 μM Arg. Increasing Arg concentrations from 50 to 400 μM had no effect on total AMPK levels but increased ($P < 0.05$) phosphorylated AMPK levels by approximately 110%, and therefore, the ratio of phosphorylated AMPK to total AMPK by 80%. Compared with 0 or 50 μM Arg, exposure of the cells to 400 μM Arg did not affect ($P > 0.05$) total or phosphorylated levels of ACC, or the ratio of phosphorylated ACC to total ACC.

C2C12 skeletal muscle cells

In C2C12 myotubes, increasing extracellular concentrations of Arg from 0 to 50 μM increased ($P < 0.05$) oleic acid oxidation but had no effect ($P > 0.05$) on glucose oxidation or lactate production (Table 2). Increasing Arg concentration from 50 to 400 μM increased ($P < 0.05$) glucose oxidation and lactate production, but had no effect ($P > 0.05$) on oleic acid oxidation. The rate of oleic acid oxidation was 23% greater ($P < 0.05$) in the presence of

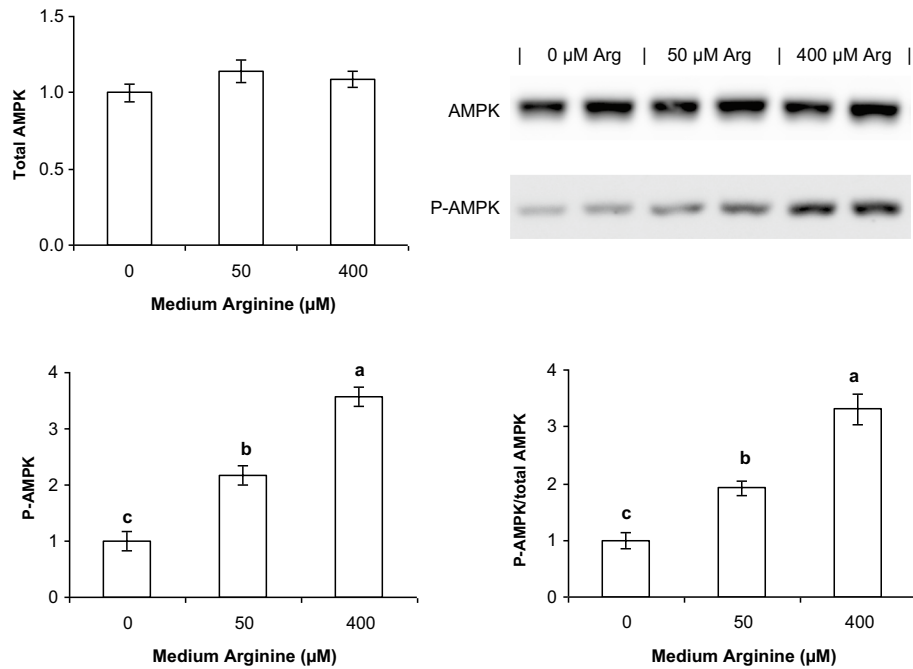


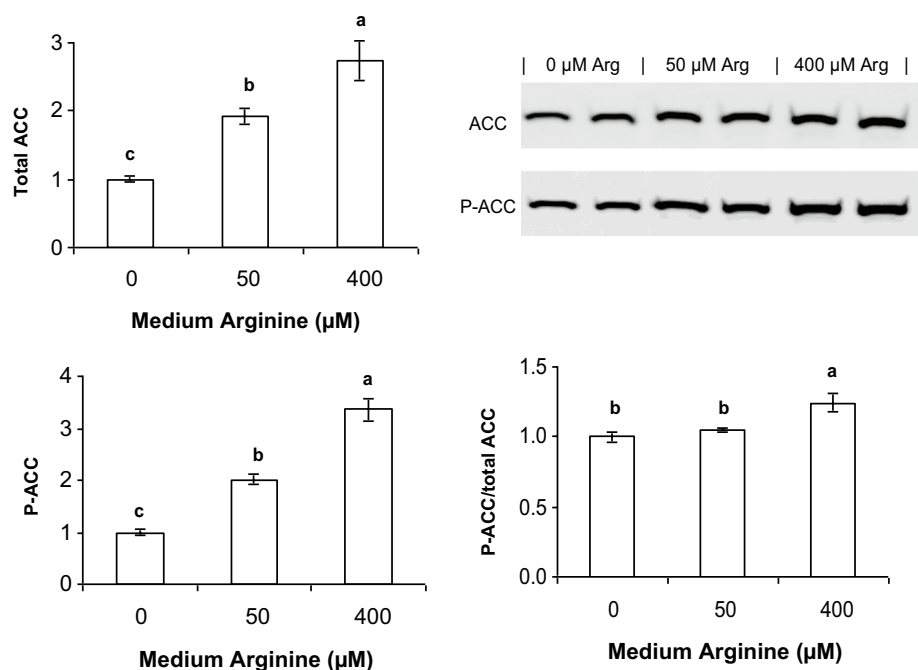
Fig. 3 Relative protein levels for total AMPK α , phosphorylated AMPK α (P-AMPK α) and the ratio of P-AMPK α to total AMPK α in C2C12 myotubes. Cells were cultured for 48 h in customized DMEM containing 0, 50 or 400 μ M L-arginine. The same amount of cell proteins (30 μ g) from different treatment groups was loaded into 4–12% SDS–polyacrylamide gels for the separation of AMPK α and phos-

phorylated AMPK α proteins. The protein images were developed with the use of the Supersignal West Dura Extended Duration Substrate, and two representative blots from each treatment group are shown. Data, expressed as relative values to the cells cultured without added L-arginine, are means \pm SEM, $n=4$. Means with different letters are different ($P<0.05$)

400 μ M Arg than in the absence of its addition. In C2C12 cells cultured in the presence or absence of Arg, the rate of lactate production from glucose was much greater than the rate of glucose oxidation to CO₂.

Staining intensities of total proteins bound to the blotting membrane for C2C12 cells cultured with 0, 50, and 400 μ M Arg were 1.000 ± 0.033 , 0.983 ± 0.036 , and 1.025 ± 0.041 AU, respectively ($P>0.05$). Increasing extracellular

Fig. 4 Relative protein levels for total ACC, phosphorylated ACC (P-ACC) and the ratio of P-ACC to total ACC in C2C12 myotubes. Cells were cultured for 48 h in customized DMEM containing 0, 50 or 400 μ M L-arginine. The same amount of cell proteins (30 μ g) from different treatment groups was loaded into 4–12% SDS–polyacrylamide gels for the separation of ACC and phosphorylated ACC proteins. The protein images were developed with the use of the Supersignal West Dura Extended Duration Substrate, and two representative blots from each treatment group are shown. Data, expressed as relative values to the cells cultured without added L-arginine, are means \pm SEM, $n=4$. Means with different letters are different ($P<0.05$)



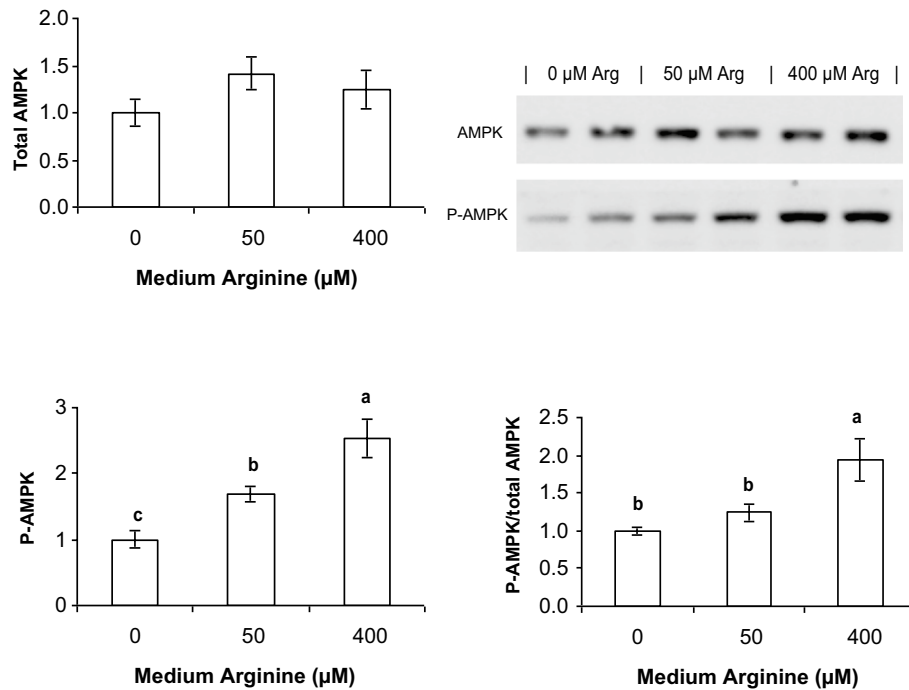


Fig. 5 Relative protein levels for total AMPK α , phosphorylated AMPK α (P-AMPK α) and the ratio of P-AMPK α to total AMPK α in 3T3-L1 adipocytes. Cells were cultured for 48 h in customized DMEM containing 0, 50 or 400 μ M L-arginine. The same amount of cell proteins (30 μ g) from different treatment groups was loaded into 4–12% SDS–polyacrylamide gels for the separation of

AMPK α and phosphorylated AMPK α proteins. The protein images were developed with the use of the Supersignal West Dura Extended Duration Substrate, and two representative blots from each treatment group are shown. Data, expressed as relative values to the cells cultured without added L-arginine, are means \pm SEM, $n=4$. Means with different letters are different ($P<0.05$)

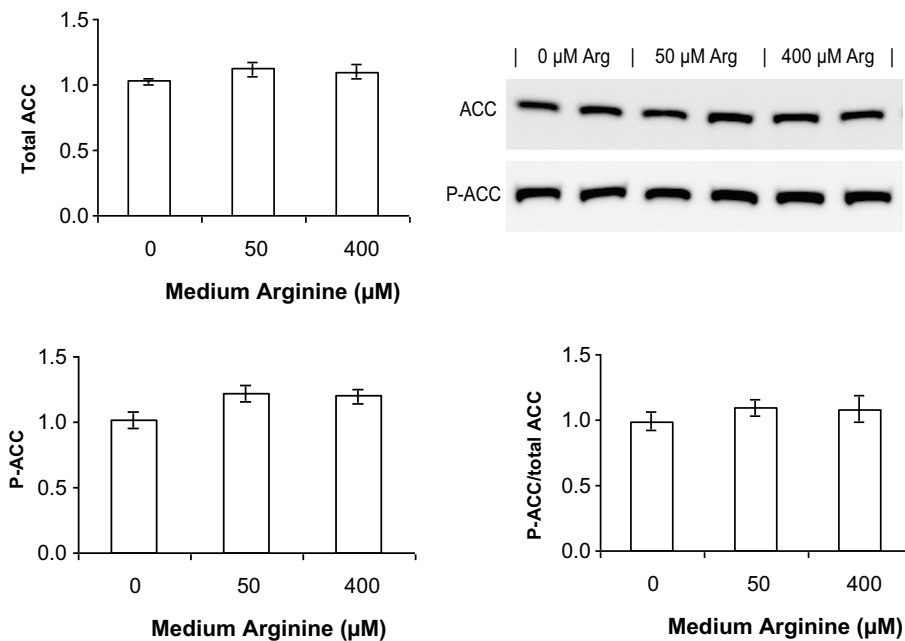


Fig. 6 Relative protein levels for total ACC, phosphorylated ACC (P-ACC) and the ratio of P-ACC to total ACC in 3T3-L1 adipocytes. Cells were cultured for 48 h in customized DMEM containing 0, 50 or 400 μ M L-arginine. The same amount of cell proteins (30 μ g) from different treatment groups was loaded into 4–12% SDS–polyacrylamide gels for the separation of ACC and phosphorylated ACC

proteins. The protein images were developed with the use of the Supersignal West Dura Extended Duration Substrate, and two representative blots from each treatment group are shown. Data, expressed as relative values to the cells cultured without added L-arginine, are means \pm SEM, $n=4$. Means for each measured variable are not different ($P>0.05$) among the three concentrations of Arg

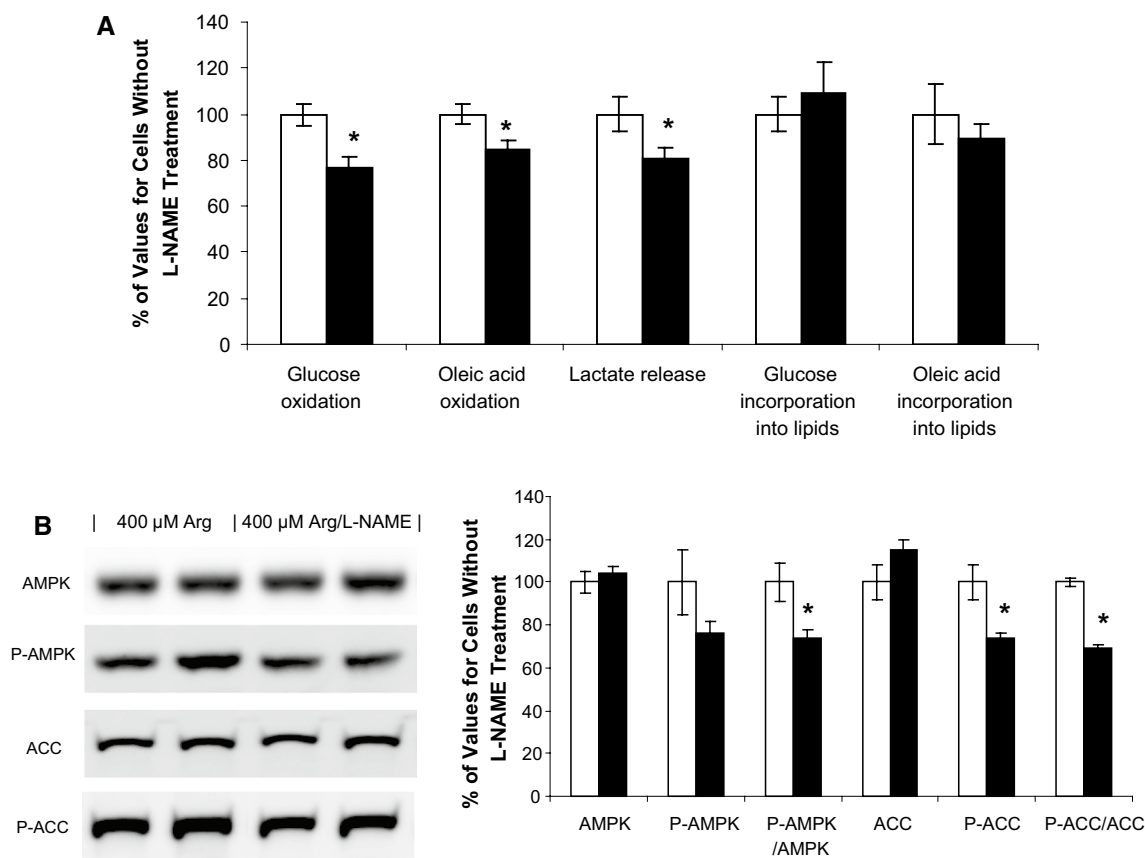


Fig. 7 The effect of L-NAME on glucose and oleic acid oxidation, lactate release, the incorporations of glucose into lipids, and the incorporation of oleic acid into esterified lipids (A), as well as total and phosphorylated levels of AMPK α and ACC (B) in BNL CL.2 hepatocytes. Cells were cultured for 48 h in customized DMEM containing either 400 μ M L-arginine (open bars) or 400 μ M L-arginine plus 0.5 mM L-NAME (black bars). The same amount of cell proteins (30 μ g) from different treatment groups was loaded into 4–12%

SDS–polyacrylamide gels for the separation of AMPK α and phosphorylated AMPK α proteins, as well as ACC and phosphorylated ACC proteins. The protein images were developed with the use of the Supersignal West Dura Extended Duration Substrate, and two representative blots from each treatment group are shown. Data, expressed as relative values to the cells cultured without added L-arginine, are means \pm SEM, $n=5$ for biochemical assays and $n=4$ for western blots. * $P<0.05$: Different from the group without L-NAME

concentrations of Arg from 0 to 50 and 400 μ M had no effect ($P>0.05$) on total AMPK levels in C2C12 myotubes but progressively increased ($P<0.05$) phosphorylated AMPK levels by 117% and 256%, respectively, and thus the ratio of phosphorylated AMPK to total AMPK by 92% and 231%, respectively (Fig. 3). Arg at 50 μ M increased ($P<0.05$) both total ACC and phosphorylated ACC levels approximately by 100%, as compared with 0 μ M Arg. Arg at 400 μ M further increased ($P<0.05$) total ACC and phosphorylated ACC levels by 174% and 236%, respectively, in comparison with the values obtained at 0 μ M Arg. As a result, the ratio of phosphorylated ACC to ACC was not changed ($P>0.05$) by 50 μ M Arg, but was increased ($P<0.05$) by 400 μ M Arg in C2C12 cells (Fig. 4).

3T3-L1 adipocytes

Table 3 summarizes the effect of Arg on glucose and oleic acid metabolism in 3T3-L1 cells. Lactate was the major product of glucose metabolism in adipocytes. Increasing extracellular concentrations of Arg from 0 up to 400 μ M did not affect ($P>0.05$) lactate production or the incorporation of glucose into lipids in these cells. The rates of glucose oxidation in 3T3-L1 cells did not differ ($P>0.05$) between 0 and 100 μ M Arg, but were 45% greater ($P<0.05$) in the presence of 400 μ M Arg than in the absence of its addition. Incorporation into esterified lipids was the major fate (80–90%) of oleic acid utilization by 3T3-L1 cells. Increasing extracellular concentrations of Arg from 0 to 50 μ M had no effect ($P>0.05$) on the oxidation of oleic acid or its incorporation into esterified lipids in these cells. However, the rates of oleic acid oxidation in 3T3-L1 cells

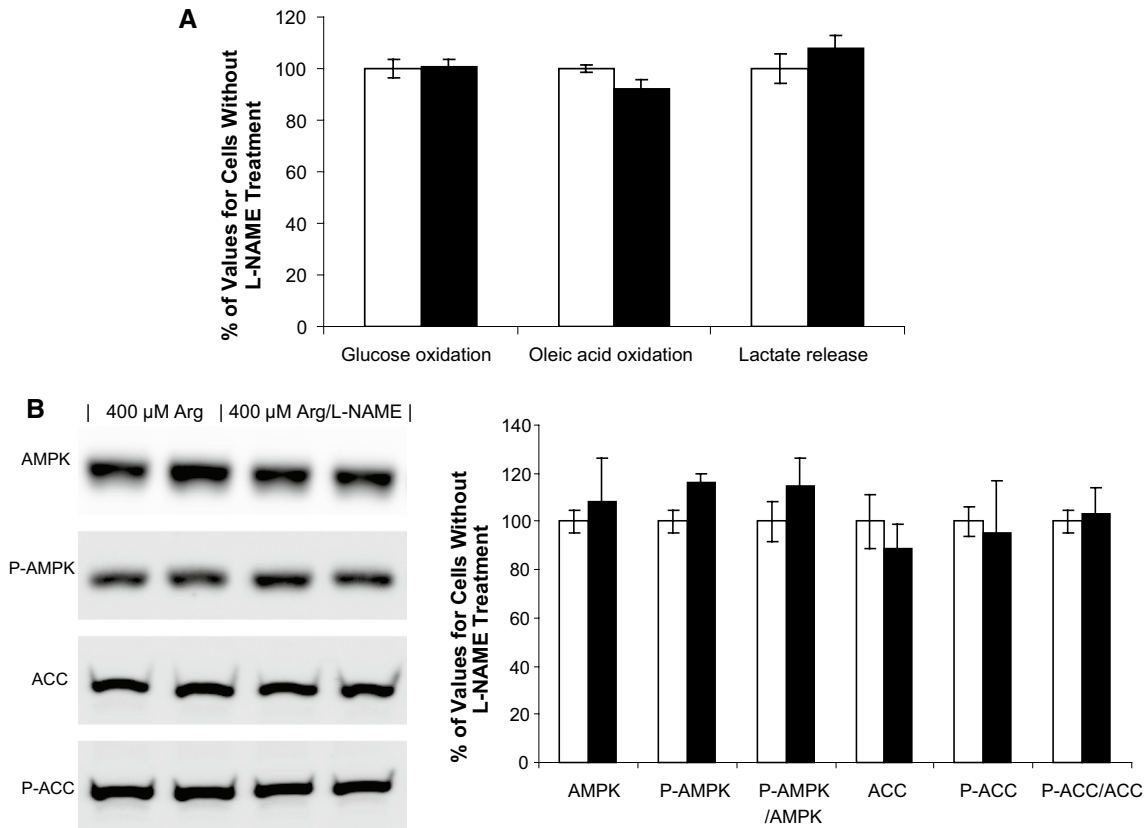


Fig. 8 The effect of L-NAME on glucose and oleic acid oxidation, lactate release, the incorporations of glucose into lipids, and the incorporation of oleic acid into esterified lipids (A), as well as total and phosphorylated levels of AMPK α and ACC (B) in C2C12 myotubes. Cells were cultured for 48 h in customized DMEM containing either 400 μ M L-arginine (open bars) or 400 μ M L-arginine plus 0.5 mM L-NAME (black bars). The same amount of cell proteins (30 μ g) from different treatment groups was loaded into 4–12% SDS–polyacrylamide gels for the separation of AMPK α and phos-

phorylated AMPK α proteins, as well as ACC and phosphorylated ACC proteins. The protein images were developed with the use of the Supersignal West Dura Extended Duration Substrate, and two representative blots from each treatment group are shown. Data, expressed as relative values to the cells cultured without added L-arginine, are means \pm SEM, $n=6$ for biochemical assays and $n=4$ for western blots. Inhibition of NO synthesis by L-NAME did not affect ($P > 0.05$) the measured variables in C2C12 cells

were approximately 40% greater ($P < 0.05$) in the presence of 100–400 μ M Arg than in its absence. Also, increasing Arg concentration from 50 to 100 and 400 μ M increased ($P < 0.05$) the incorporation of oleic acid into esterified lipids in these cells by 136% and 190%, respectively.

Staining intensities of total proteins bound to the blotting membrane for 3T3-L1 cells cultured with 0, 50, and 400 μ M Arg were 1.000 ± 0.037 , 1.045 ± 0.049 , and 1.040 ± 0.053 AU, respectively ($P > 0.05$). Increasing extracellular concentrations of Arg from 0 to 400 μ M did not affect ($P > 0.05$) total AMPK but increased ($P < 0.05$) phosphorylated AMPK levels. Arg at 400 μ M increased ($P < 0.05$) the ratio of phosphorylated AMPK to total AMPK by approximately 90% compared to 0 μ M Arg (Fig. 5). In contrast, increasing Arg concentrations from 0 to 400 μ M had no effect ($P > 0.05$) on total or phosphorylated ACC levels, or the ratio of phosphorylated ACC to total ACC in 3T3-L1 adipocytes (Fig. 6).

NO synthesis by BNL CL.2, C2C12, and 3T3-L1 cells

Increasing extracellular concentrations of Arg from 0 to 400 μ M did not affect ($P > 0.05$) nitrite production in 3T3-L1 cells (Table 4). In both BNL CL.2 and C2C12 cells, nitrite production did not differ ($P > 0.05$) between 0 and 100 μ M Arg (Table 4). However, rates of NO synthesis were 42% and 47% greater ($P < 0.05$) in the presence of 400 μ M Arg than in its absence in BNL CL.2 and C2C12 cells, respectively. The addition of 0.5 mM L-NAME to culture medium inhibited the production of NO in the three cell lines by approximately 80% (Table 4).

Effect of L-NAME on BNL CL.2, C2C12 and 3T3-L1 cells

Addition of 0.5 mM L-NAME to culture media reduced ($P < 0.05$) glucose oxidation, oleic acid oxidation and

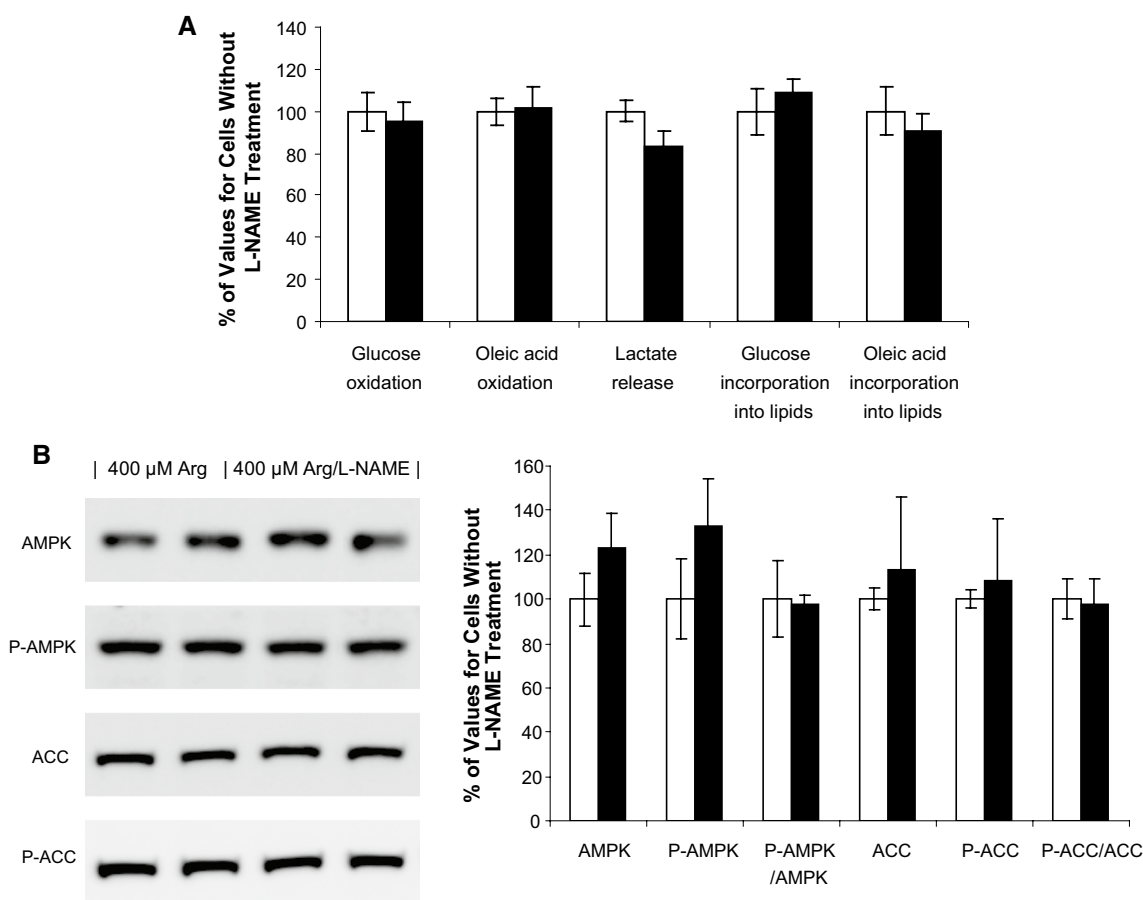


Fig. 9 The effect of L-NAME on glucose and oleic acid oxidation, lactate release, the incorporations of glucose into lipids, and the incorporation of oleic acid into esterified lipids (A), as well as total and phosphorylated levels of AMPK α and ACC (B) in 3T3-L1 adipocytes. Cells were cultured for 48 h in customized DMEM containing either 400 μ M L-arginine (open bars) or 400 μ M L-arginine plus 0.5 mM L-NAME (black bars). The same amount of cell proteins (30 μ g) from different treatment groups was loaded into 4–12% SDS-polyacrylamide gels for the separation of AMPK α and phosphoryl-

ated AMPK α proteins, as well as ACC and phosphorylated ACC proteins. The protein images were developed with the use of the Supersignal West Dura Extended Duration Substrate, and two representative blots from each treatment group are shown. Data, expressed as relative values to the cells cultured without added L-arginine, are means \pm SEM, $n=5$ for biochemical assays and $n=4$ for western blots. Inhibition of NO synthesis by L-NAME did not affect ($P > 0.05$) the measured variables in 3T3-L1 adipocytes

lactate production by approximately 20% in BNL CL.2 cells but had no effect ($P > 0.05$) on the incorporation of glucose into lipids and of oleic acid into esterified lipids, compared with the absence of the NOS inhibitor (Fig. 7A). Staining intensities of total proteins bound to the blotting membrane for BNL CL.2 cells cultured with 400 μ M Arg and 400 μ M Arg + 0.5 mM L-NAME were 1.000 ± 0.047 and 1.028 ± 0.042 AU, respectively; those for C2C12 cells were 1.000 ± 0.042 and 1.035 ± 0.051 AU, respectively ($P > 0.05$); and those for 3T3-L1 cells were 1.000 ± 0.044 and 0.993 ± 0.037 AU, respectively ($P > 0.05$). L-NAME treatment did not affect ($P > 0.05$) total or phosphorylated AMPK levels, but reduced ($P < 0.05$) the ratio of phosphorylated AMPK to total AMPK. Total ACC levels were not altered ($P > 0.05$) by 0.5 mM L-NAME, but both phosphorylated ACC levels and the ratio of phosphorylated ACC

to total ACC in hepatocytes were reduced ($P < 0.05$) by L-NAME treatment (Fig. 7B). In C2C12 myotubes (Fig. 8) or 3T3-L1 adipocytes (Fig. 9), 500 μ M L-NAME did not affect ($P > 0.05$) glucose oxidation, oleic acid oxidation, lactate release, or protein levels for AMPK and ACC.

Discussion

Plasma concentrations of Arg in healthy overnight-fasted and fed adults are approximately 100 and 200 μ M, respectively (Wu and Morris 1998; Wu et al. 2004a). Dietary supplementation with 1% Arg to animals can increase plasma Arg concentrations to about 500 μ M (Wu et al. 2007, 1999). Interestingly, as low as 15 and 30 μ M Arg are present in the plasma of liver-transplant recipients (Reid et al. 2007) and

Table 1 Glucose and oleic acid metabolism in BNL CL.2 hepatocytes

Variables	Medium L-arginine concentrations (μM)					P value
	0	15	50	100	400	
Glucose oxidation (nmol glucose/mg protein per h)	24.5 \pm 2.2 ^c	31.6 \pm 0.84 ^c	33.6 \pm 3.2 ^{b,c}	42.9 \pm 2.3 ^{a,b}	53.2 \pm 2.5 ^a	0.0005
Oleic acid oxidation (nmol oleic acid/mg protein per h)	0.99 \pm 0.05 ^b	1.01 \pm 0.07 ^b	1.10 \pm 0.05 ^b	1.74 \pm 0.11 ^a	2.08 \pm 0.12 ^a	0.0005
Lactate release (nmol lactate/mg protein per h)	218 \pm 16	218 \pm 34	207 \pm 10	262 \pm 29	250 \pm 19	0.49
Glucose incorporation into lipids (nmol glucose/mg protein per h)	0.85 \pm 0.04	1.01 \pm 0.13	0.96 \pm 0.06	1.08 \pm 0.09	0.82 \pm 0.09	0.23
Oleic acid incorporation into esterified lipids (nmol oleic acid/mg protein per h)	7.73 \pm 0.81 ^b	6.18 \pm 0.81 ^b	8.39 \pm 1.53 ^b	15.92 \pm 1.31 ^a	18.89 \pm 2.51 ^a	0.0005

Cells were incubated for 48 h in customized DMEM containing 0, 15, 50, 100 or 400 μM L-arginine. Data are expressed as means \pm SEM, $n = 5$

^{a-c}Means with different superscript letters in a row are different ($P < 0.05$)

Table 2 Glucose and oleic acid metabolism in C2C12 myotubes

Variables	Medium L-arginine concentrations (μM)					P value
	0	15	50	100	400	
Glucose oxidation (nmol glucose/mg protein per h)	11.5 \pm 0.4 ^c	11.3 \pm 0.4 ^c	13.4 \pm 1.1 ^c	18.6 \pm 1.0 ^b	22.3 \pm 0.9 ^a	0.0005
Oleic acid oxidation (nmol oleic acid/mg protein per h)	1.46 \pm 0.08 ^b	1.66 \pm 0.03 ^{ab}	1.75 \pm 0.08 ^a	1.72 \pm 0.08 ^a	1.80 \pm 0.03 ^a	0.030
Lactate release (nmol lactate/mg protein per h)	176 \pm 10 ^b	196 \pm 7.8 ^b	251 \pm 11 ^b	436 \pm 29 ^a	453 \pm 26 ^a	0.0005

Cells were incubated for 48 h in customized DMEM containing 0, 15, 50, 100 or 400 μM L-arginine. Data are expressed as means \pm SEM, $n = 6$

^{a-c}Means with different superscript letters in a row are different ($P < 0.05$)

Table 3 Glucose and oleic acid metabolism in 3T3-L1 adipocytes

Variables	Medium L-arginine concentrations (μM)					P value
	0	15	50	100	400	
Glucose oxidation (nmol glucose/mg protein per h)	12.1 \pm 0.4 ^b	14.4 \pm 1.2 ^{a,b}	15.5 \pm 1.3 ^{a,b}	16.1 \pm 0.9 ^{a,b}	17.6 \pm 1.6 ^a	0.037
Oleic acid oxidation (nmol oleic acid/mg protein per h)	1.77 \pm 0.07 ^c	2.04 \pm 0.08 ^{b,c}	2.12 \pm 0.10 ^{a,b,c}	2.40 \pm 0.09 ^{a,b}	2.48 \pm 0.16 ^a	0.001
Lactate release (nmol lactate/mg protein per h)	197 \pm 17	184 \pm 5	204 \pm 17	200 \pm 5	203 \pm 10	0.78
Glucose incorporation into lipids (nmol glucose/mg protein per h)	9.54 \pm 0.53	11.1 \pm 0.74	9.35 \pm 0.43	11.0 \pm 0.44	9.73 \pm 1.05	0.25
Oleic acid incorporation into esterified lipids (nmol oleic acid/mg protein per h)	6.40 \pm 1.12 ^b	6.88 \pm 1.98 ^b	10.9 \pm 1.38 ^b	25.7 \pm 3.64 ^a	31.6 \pm 3.05 ^a	0.0005

Cells were incubated for 48 h in customized DMEM containing 0, 15, 50, 100 or 400 μM of L-arginine. Data are expressed as means \pm SEM, $n = 5$

^{a-c}Means with different superscript letters in a row are different ($P < 0.05$)

preterm infants (Wu et al. 2004b), due to the release of arginase from the liver and the underdevelopment of endogenous Arg synthesis pathways, respectively. In contrast, porcine allantoic fluid contains 4–6 mM Arg during early gestation (Wu et al. 1996, 1998). Thus, the concentrations of Arg used in the present study (15–400 μM) are within the physiological and pathological ranges found in mammals, and the findings are of nutritional and clinical relevance.

Arg enters mammalian cells via cationic amino acid transporters (Closs et al. 2006). Much evidence shows that increasing extracellular concentrations of Arg augments

its intracellular concentrations (Wu and Meininger 2002). In BNL CL.2 hepatocytes, C2C12 myotubes and 3T3-L1 adipocytes, glucose and oleic acid oxidation increased in response to elevated extracellular concentrations of Arg from 0 to 400 μM (Tables 1, 2 and 3), indicating a role for Arg in stimulating energy substrate oxidation in these cells. In addition, the Arg treatment enhanced glycolysis in skeletal muscle cells, as indicated by the increased production of lactate (Table 2). These results were consistent with the findings of the previous in vivo studies that dietary Arg supplementation increased the metabolism of energy substrates

Table 4 The effect of L-arginine on nitrite production in BNL CL.2, C2C12 and 3T3-L1 cells

Nitrite (pmol/mg protein per 24 h)	Medium L-arginine concentrations (nM)				400 μ M L-Arginine + 0.5 mM L-NAME	P value
	0	50	100	400		
BNL CL.2	112 \pm 12 ^b	119 \pm 10 ^b	125 \pm 13 ^b	159 \pm 4 ^a	31 \pm 1.5 ^c	<0.01
C2C12	351 \pm 19 ^b	372 \pm 61 ^b	363 \pm 15 ^b	516 \pm 41 ^a	105 \pm 3.8 ^c	<0.01
3T3-L1	200 \pm 18 ^a	207 \pm 1 ^a	232 \pm 28 ^a	264 \pm 27 ^a	50 \pm 1.7 ^b	<0.01

Cells were incubated for 48 h in customized DMEM containing 0, 15, 50, 100 or 400 μ M of L-arginine. Culture medium containing 400 μ M L-arginine also included 0.5 mM L-NAME. Culture medium was changed every 24 h. At the end of the 48-h culture period, the conditioned media were analyzed for nitrite

Data are expressed as means \pm SEM, $n=5$

^{a-c}Means with different superscript letters in a row are different ($P < 0.05$)

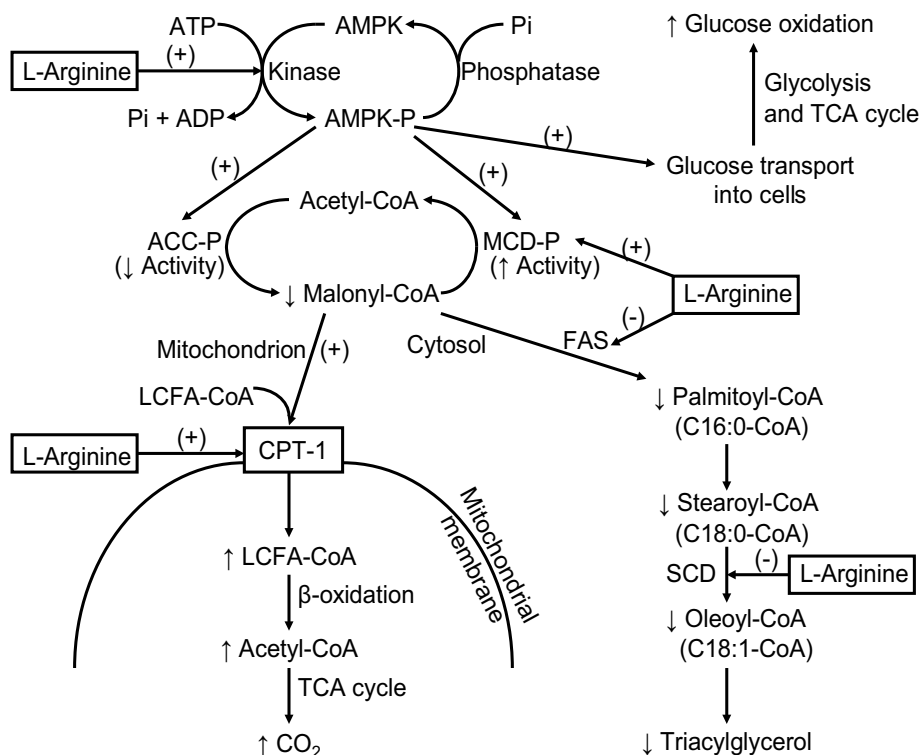


Fig. 10 The proposed mechanisms responsible for the beneficial effect of L-arginine on the oxidation of energy substrates and the synthesis of triacylglycerol in animals. Physiological concentrations of L-arginine stimulate the phosphorylation of AMPK, which then phosphorylates ACC and malonyl-CoA decarboxylase. This results in the inactivation of ACC [and thus a reduction in the generation of malonyl-CoA (an inhibitor of CPT-I) from acetyl-CoA], as well as the activation of malonyl-CoA decarboxylase [and thus an increase in the conversion of malonyl-CoA into CO₂ and acetyl-CoA], leading to a decrease in intracellular concentrations of malonyl-CoA. In addition, activated AMPK stimulates the transport of glucose primarily

by skeletal muscle, hepatocytes, and white adipocytes. Consequently, L-arginine enhances the activity of CPT-I and the oxidation of long-chain fatty acids to CO₂, as well as the oxidation of glucose to CO₂, in insulin-sensitive tissues. The symbol (+) denotes an increase in gene expression and/or enzyme activation. The symbol (-) denotes an inhibition of gene expression and/or enzyme activity. ACC acetyl-CoA carboxylase, AMPK AMP-activated protein kinase, CPT-I carnitine palmitoyltransferase I, LCFA long-chain fatty acids, MCD malonyl-CoA decarboxylase, SCD-1 stearoyl-CoA desaturase 1, TCA tricarboxylic acid

in the skeletal muscle and adipose tissue of obese rats (Fu et al. 2005; Jobgen 2007), as well whole-body glucose oxidation and insulin sensitivity in obese men (Boon et al. 2019). Because the BNL CL.2, C2C12, and 3T3-L1 cells

were derived from the fetal mouse liver, the dystrophic adult mouse skeletal muscle, and the mouse embryonic fibroblast (Kuppusamy et al. 2021; Muller and Danner 2004), these cell lines may differ from the hepatocytes, skeletal muscle,

and white adipocytes of rats in both metabolism and cells signaling.

We found that phosphorylated AMPK levels in all the three cell types used in the present study were increased in response to an increase in extracellular concentrations of Arg from 0 to 400 μM (Figs. 1, 3 and 5), as reported for AMPK activation in the liver of diet-induced obese rats receiving dietary supplementation with Arg (Jobgen and Wu 2022). This result may provide a mechanism for explaining the increased oxidation of glucose and fatty acids in Arg-treated hepatocytes, skeletal muscle cells and adipocytes, on the basis of the previous reports that AMPK phosphorylation promotes substrate oxidation in insulin-sensitive cells (Kahn et al. 2005a, b). Also, in C2C12 cells, elevated levels of phosphorylated ACC, a downstream target of AMPK, increased in response to Arg supplementation, leading to reductions in ACC enzymatic activity and, therefore, the generation of malonyl-CoA [a potent inhibitor of carnitine palmitoyltransferase I (CPT-I)] from acetyl-CoA. In addition, phosphorylated AMPK stimulates malonyl-CoA decarboxylase, resulting in the increased conversion of malonyl-CoA into CO_2 and acetyl-CoA (Ruderman and Prentki 2004). Thus, the inactivation of ACC and the activation of malonyl-CoA decarboxylase via their phosphorylation will lead to a decrease in intracellular concentrations of malonyl-CoA and, consequently, an increase in the activity of CPT-I (Viollet et al. 2006), thereby facilitating the transport of long-chain fatty acids from the cytosol to mitochondria for oxidation into CO_2 in Arg-treated C2C12 cells.

Arg is catabolized by multiple pathways to form NO, ornithine, and proline in cultured cells (Wu and Morris 1998). The addition of 0.1 mM ornithine plus proline (the major products of Arg catabolism via the arginase pathway) to culture medium had no effect on glucose or oleic acid oxidation in endothelial cells or enterocytes (our unpublished data). These results suggest that ornithine or proline do not mediate the effect of Arg on metabolism in these cell types. Whether ornithine and proline affect substrate metabolism in BNL CL.2 hepatocytes, C2C12 myotubes and 3T3-L1 adipocytes remains to be determined.

As a stimulator of mitochondrial biogenesis, a vasodilator, and cell signaling molecule, NO has been suggested to modulate energy metabolism, fat deposition in white adipocytes, and insulin resistance in mammals including humans (Sansbury and Hill 2014) and rats (McKnight et al. 2010; Peyton et al. 2018; Wu 2022). Interestingly, increasing extracellular concentrations of Arg from 0 to 400 μM increased NO synthesis in BNL CL.2 cells, as reported for Arg-treated rat hepatocytes (Morita et al. 1996). However, an inhibition of NO synthesis by ~80% (Table 4) only moderately attenuated the effect of Arg on the phosphorylation of AMPK and ACC as well as glucose oxidation, glycolysis, and oleic acid oxidation in BNL CL.2 cells (Fig. 4). This

result is consistent with the report that NO or cGMP can stimulate fatty acid oxidation through reducing ACC activity and enhancing CPT-I activity in rat hepatocytes (Garcia-Villafranca et al. 2003). However, an inhibition of NO synthesis had no effect on AMPK and ACC phosphorylation or glucose and oleic acid metabolism in C2C12 skeletal muscle cells and 3T3-L1 adipocytes (Figs. 5 and 6). These findings suggest that, under the experimental conditions used in the present study where culture medium contained 500 μM L-glutamine to reduce NO synthesis (Meininger and Wu 1997; Houdijk et al. 1998; Wu et al. 2001), NO was not a major regulator of AMPK and ACC activity or the oxidation of energy substrates in the three cell lines used in the present study. Consistent with this view are the following observations. First, NO synthesis in 3T3-L1 cells did not differ between 0 and 400 μM Arg (Table 4). Second, increasing extracellular concentrations of Arg from 0 to 100 μM increased glucose and oleic acid oxidation in BNL CL.2 cells (Table 1) and C2C12 cells (Table 2) but did not affect NO production in these two cell types (Table 4). It is possible that Arg catabolism is not necessary for exerting its stimulatory effect on substrate oxidation in hepatocytes, adipocytes and muscle cells and that Arg may directly activate AMPK in a cell-specific manner. In support of this notion, previous studies have shown that Arg can directly increase the expression of GTP cyclohydrolase-I in endothelial cells (Shi et al. 2004) and stimulate mTOR phosphorylation in intestinal cells (Rhoads et al. 2007).

In both BNL CL.2 hepatocytes and 3T3-L1 adipocytes, Arg increased the incorporation of oleic acid into esterified lipids. Liver and white adipose tissue are the two major sites for de novo fatty acid synthesis in rodents (Bergen and Mersmann 2005; Kalupahana et al. 2010). Because high concentrations of free long-chain fatty acids are toxic to cells (Jobgen et al. 2006), an increase in their packaging into esterified lipids may have important implications for cell integrity and the regulation of plasma concentrations of free fatty acids. This may help explain the finding that dietary Arg supplementation reduced the circulating levels of free fatty acids in ZDF rats (Fu et al. 2005) and serum concentrations of triglycerides in diet-induced obese rats (Jobgen et al. 2009). The proposed mechanisms for the beneficial effects of Arg on reducing white adipose tissue are summarized in Fig. 10. Because the liver is the principal organ for both de novo fatty acid synthesis and fatty acid oxidation in rats and humans (Bergen and Mersmann 2005), augmentation in the esterification of long-chain fatty acids into triacylglycerols, an inhibition of fatty acid synthesis, and an increase in fatty acid oxidation in hepatocytes provide a key molecular basis for the anti-obesity effect of Arg. These findings indicate that dietary supplementation with Arg coordinately regulates the expression of key genes and activity of proteins that are involved

in the metabolism of energy substrates, thereby reducing excessive fat and improving insulin sensitivity in diet-induced obese rats.

In summary, results of the present study demonstrate that Arg enhances glucose and oleic acid oxidation in BNL CL2 hepatocytes, C2C12 myotubes, and 3T3-L1 adipocytes in association with increased AMPK phosphorylation. These effects of Arg were mediated only to a small extent by an NO-dependent mechanism in BNL CL2 cells and was independent of NO production in C2C12 and 3T3-L1 cells. We suggest that Arg itself may directly activate AMPK, thereby stimulating the oxidation of energy substrates in insulin-sensitive cells. Future experiments with AMPK inhibitors are warranted to test this hypothesis.

Acknowledgements We thank Dr. Stephen B. Smith and Dr. Cynthia J. Meininger for helpful discussions, as well as Mr. Scott Jobgen for assistance in laboratory analyses of metabolites. This research was supported by grants from American Heart Association–Texas (#0755024Y and 10GRNT4480020).

Declarations

Conflict of interest The authors declare that they have no conflict of interest.

Ethics statement Established cell lines available from commercial companies were used for this study. Thus, the present work did not require the approval for the use of animals by Institutional Animal Care and Use Committee of Texas A&M University.

Informed consent No informed consent is required for this study.

References

- Alam MA, Kauter K, Withers K, Sernia C, Brown L (2013) Chronic L-arginine treatment improves metabolic, cardiovascular and liver complications in diet-induced obesity in rats. *Food Funct* 4:83–91
- Alderton WK, Cooper CE, Knowles RG (2001) Nitric oxide synthases: structure, function and inhibition. *Biochem J* 357:593–615
- Assaad H, Zhou L, Carroll RJ, Wu G (2014) Rapid publication-ready MS word tables for one-way ANOVA. Springer plus 3:474
- Bergen W, Mersmann HJ (2005) Comparative aspects of lipid metabolism: impact on contemporary research and use of animal models. *J Nutr* 135:2499–2502
- Boon MR, Hanssen MJW, Brans B, Hülsman CJM, Hoeks J, Nahon KJ, Bakker C, van Klinken JB, Havekes B, Schaart G, Jazet IM, Rensen PCN, van Marken Lichtenbelt WD (2019) Effect of L-arginine on energy metabolism, skeletal muscle and brown adipose tissue in South Asian and European prediabetic men: a randomised double-blinded crossover study. *Diabetologia* 62:112–122
- Ceddia RB, William WN Jr, Lima FB, Flandin P, Curi R, Giacobino JP (2000) Leptin stimulates uncoupling protein-2 mRNA expression and Krebs cycle activity and inhibits lipid synthesis in isolated rat white adipocytes. *Eur J Biochem* 267:5952–5958
- Wu G, Jaeger LA, Bazer FW, Rhoads JM (2004b) Arginine deficiency in preterm infants: biochemical mechanisms and nutritional implications. *J Nutr Biochem* 15:442–451
- Chen JQ, Ma XS, Yang Y, Dai ZL, Wu ZL, Wu G (2018) Glycine enhances expression of adiponectin and IL-10 in 3T3-L1 adipocytes without affecting adipogenesis and lipolysis. *Amino Acids* 50(5):629–640. <https://doi.org/10.1007/s00726-018-2537-3>
- Closs EI, Boissel JP, Habermeier A, Rotmann A (2006) Structure and function of cationic amino acid transporters (CATs). *J Membr Biol* 213:67–77
- Dai ZL, Wu ZL, Yang Y, Wang JJ, Satterfield MC, Meininger CJ, Bazer FW, Wu G (2013) Nitric oxide and energy metabolism in mammals. *BioFactors* 39:383–391
- Denninger JW, Marletta MA (1999) Guanylate cyclase and the NO/cGMP signaling pathway. *Biochim Biophys Acta* 1411:334–350
- Dole VP, Meinertz H (1960) Microdetermination of long-chain fatty acids in plasma and tissues. *J Biol Chem* 235:2595–2599
- Durante W (2020) Amino acids in circulatory function and health. *Adv Exp Med Biol* 1265:39–56
- Förstermann U, Sessa WC (2012) Nitric oxide synthases: regulation and function. *Eur Heart J* 33:829–837
- Förstermann U, Closs EI, Pollock JS, Nakane M, Schwarz P, Gath I, Kleinert H (1994) Nitric oxide synthase isozymes. Characterization, purification, molecular cloning, and functions. *Hypertension* 23:1121–1131
- Fouad AM, El-Senousey HK, Yang XJ, Yao JH (2013) Dietary L-arginine supplementation reduces abdominal fat content by modulating lipid metabolism in broiler chickens. *Animal* 7:1239–1245
- Fu WJ, Haynes TE, Kohli R, Hu J, Shi W, Spencer TE, Carroll RJ, Meininger CJ, Wu G (2005) Dietary L-arginine supplementation reduces fat mass in Zucker diabetic fatty rats. *J Nutr* 135:714–721
- Wu G, Bazer FW, Cudd TA, Jobgen WS, Kim SW, Lassala A, Li P, Matis JH, Meininger CJ, Spencer TE (2007) Pharmacokinetics and safety of arginine supplementation in animals. *J Nutr* 137:1673S–1680S
- Garcia-Villafraña J, Guillen A, Castro J (2003) Involvement of nitric oxide/cyclic GMP signaling pathway in the regulation of fatty acid metabolism in rat hepatocytes. *Biochem Pharmacol* 65:807–812
- He WL, Wu G (2022) Oxidation of amino acids, glucose, and fatty acids as metabolic fuels in enterocytes of developing pigs. *Amino Acids* 54(7):1025–1039. <https://doi.org/10.1007/s00726-022-03151-7>
- Houdijk APJ, Visser JJ, Rijnsburger ER, Teerlink T, van Leeuwen PAM (1998) Dietary glutamine supplementation reduces plasma nitrate levels in rats. *Clin Nutr* 17:11–14
- Jobgen WS (2007) Dietary L-arginine supplementation reduces fat mass in diet-induced obese rats. PhD Dissertation. Texas A&M University, College Station, TX, USA
- Jobgen WS, Wu G (2022) Dietary L-arginine supplementation increases the hepatic expression of AMP-activated protein kinase in rats. *Amino Acids*. <https://doi.org/10.1007/s00726-022-03194-w>
- Jobgen WS, Fried SK, Fu WJ, Meininger CJ, Wu G (2006) Regulatory role for the arginine-nitric oxide pathway in metabolism of energy substrates. *J Nutr Biochem* 17:571–588
- Jobgen WS, Jobgen SC, Li H, Meininger CJ, Wu G (2007) Analysis of nitrite and nitrate in biological samples using high-performance liquid chromatography. *J Chromatogr B* 851:71–82
- Jobgen WJ, Meininger CJ, Jobgen SC, Li P, Lee M-J, Smith SB, Spencer TE, Fried SK, Wu G (2009) Dietary L-arginine supplementation reduces white-fat gain and enhances skeletal muscle and brown fat masses in diet-induced obese rats. *J Nutr* 139:230–237
- Kahn BB, Alquier T, Carling D, Hardie DG (2005a) AMP-activated protein kinase: ancient energy gauge provides clues to modern understanding of metabolism. *Cell Metab* 1:15–25
- Kahn R, Buse J, Ferranini E, Stern M (2005b) The metabolic syndrome: time for a critical appraisal. Joint statement from the

- American Diabetes Association and the European Association for the Study of Diabetes. *Diabetologia* 48:1684–1699
- Kalupahana NS, Claycombe KJ, Newman SJ, Stewart T, Siriwardhana N, Matthan N, Lichtenstein AH, Moustaid-Moussa N (2010) Eicosapentaenoic acid prevents and reverses insulin resistance in high-fat diet-induced obese mice via modulation of adipose tissue inflammation. *J Nutr* 140:1915–1922
- Khosroshahi MZ, Asbaghi O, Moradi S, Kelishadi MR, Kaviani M, Mardani M, Jalili C (2020) The effects of supplementation with L-arginine on anthropometric indices and body composition in overweight or obese subjects: a systematic review and meta-analysis. *J Funct Foods* 71:104022
- Yan H, Aziz E, Shillabeer G, Wong A, Shanghavi D, Kermouni A, Abdel-Hafez M, Lau DC (2002) Nitric oxide promotes differentiation of rat white preadipocytes in culture. *J Lipid Res* 43:2123–2129
- Kröncke KD, Kolb-Bachofen V, Berschick B, Burkart V, Kolb H (1991) Activated macrophages kill pancreatic syngeneic islet cells via arginine-dependent nitric oxide generation. *Biochem Biophys Res Commun* 175:752–758
- Kuppusamy P, Kim D, Soundharrajan I, Hwang I, Choi KC (2021) Adipose and muscle cell co-culture system: A novel in vitro tool to mimic the in vivo cellular environment. *Biology* 10:6
- Lee BS, Kang HS, Pyun KH, Choi IP (1997) Roles of tyrosine kinases in the regulation of nitric oxide synthesis in murine liver cells: Modulation of NF-kappa B activity by tyrosine kinases. *Hepatology* 25(4):913–919. <https://doi.org/10.1002/hep.510250421>
- Li H, Meininger CJ, Wu G (2000) Rapid determination of nitrite by reversed-phase high-performance liquid chromatography with fluorescence detection. *J Chromatogr B* 746:199–207
- Li SL, Zhang YC, Liu N, Chen JQ, Guo LN, Dai ZL, Wang C, Wu ZL, Wu G (2020) Dietary L-arginine supplementation reduces lipid accretion by regulating fatty acid metabolism in Nile tilapia (*Oreochromis niloticus*). *J Anim Sci Biotechnol* 11:82
- Mariotti F (2020) Arginine supplementation and cardiometabolic risk. *Curr Opin Clin Metab Care* 23:29–34
- McKnight JR, Satterfield MC, Jobgen WS, Smith SB, Spencer TE, Meininger CJ, McNeal CJ, Wu G (2010) Beneficial effects of L-arginine on reducing obesity: potential mechanisms and important implications for human health. *Amino Acids* 39:349–357
- McNeal CJ, Meininger CJ, Wilborn CD, Tekwe CD, Wu G (2018) Safety of dietary supplementation with arginine in adult humans. *Amino Acids* 50:1215–1229
- Meininger CJ, Wu G (1997) L-Glutamine inhibits nitric oxide synthesis in bovine venular endothelial cells. *J Pharmacol Exp Ther* 281:448–453
- Miczke A, Suliburska J, Pupek-Musialik D, Ostrowska L, Jablecka A, Krejpcio Z, Skrypnik D, Bogdański P (2015) Original Article Effect of L-arginine supplementation on insulin resistance and serum adiponectin concentration in rats with fat diet. *Int J Clin Exp Med* 8:10358–10366
- Morita T, Shimada Y, Ueki H, Kanagawa A (1996) Stimulation of nitric oxide-cyclic GMP pathway by L-arginine increases the release of hepatic lipase from cultured rat hepatocytes. *Biol Pharm Bull* 19:1371–1373
- Muller EA, Danner DJ (2004) Tissue-specific translation of murine branched-chain α -ketoacid dehydrogenase kinase mRNA is dependent upon an upstream open reading frame in the 5'-untranslated region. *J Biol Chem* 279:44645–44655
- Nicholls-Grzemski FA, Tirmenstein MA, Fariss MW (1999) Time-dependent production of nitric oxide by rat hepatocyte suspensions. *Biochem Pharmacol* 57:1223–1226
- Oliveira MM, Vaughan M (1964) Incorporation of fatty acids into phospholipids of erythrocyte membranes. *J Lipid Res* 5:156–162
- Peyton KJ, Liu XM, Shebib AR, Johnson FK, Johnson RA, Durante W (2018) Arginase inhibition prevents the development of hypertension and improves insulin resistance in obese rats. *Amino Acids* 50:747–754
- Raman CS, Li H, Martasek P, Kral V, Masters BS, Poulos TL (1998) Crystal structure of constitutive endothelial nitric oxide synthase: a paradigm for pterin function involving a novel metal center. *Cell* 95:939–950
- Reid KM, Tsung A, Kaizu T, Jeyabalan G, Ikeda A, Shao L, Wu G, Murase N, Geller DA (2007) Liver I/R Injury is improved by the arginase inhibitor, N- ω -Hydroxy-Nor-L-arginine (Nor-NOHA). *Am J Physiol* 292:G512–517
- Rhoads JM, Corl BA, Harrell R, Niu X, Gatlin L, Phillips O, Blikslager A, Moesser A, Wu G, Odle J (2007) Intestinal ribosomal p70^{s6k} signaling is increased in piglet rotavirus enteritis. *Am J Physiol* 292:G913–922
- Ruderman N, Prentki M (2004) AMP kinase and malonyl-CoA targets for therapy of the metabolic syndrome. *Nat Rev Drug Discov* 3:340–351
- San Martín A, Arce-Molina R, Galaz A, Pérez-Guerra G, Felipe Barros L (2017) Nanomolar nitric oxide concentrations quickly and reversibly modulate astrocytic energy metabolism. *J Biol Chem* 292:9432–9438
- Sansbury BE, Hill BG (2014) Regulation of obesity and insulin resistance by nitric oxide. *Free Radic Biol Med* 73:383–399
- Satterfield MC, Dunlap KA, Keisler DH, Bazer FW, Wu G (2012) Arginine nutrition and fetal brown adipose tissue development in diet-induced obese sheep. *Amino Acids* 43:1593–1603
- Schuman EM, Madison DV (1991) A requirement for the intercellular messenger nitric oxide in long-term potentiation. *Science* 254:1503–1506
- Sellmann C, Degen C, Jin CJ, Nier A, Engstler AJ, Alkhatib DH, De Bandt J-P, Bergheim I (2017) Oral arginine supplementation protects female mice from the onset of non-alcoholic steatohepatitis. *Amino Acids* 49:1215–1225
- Shi W, Meininger CJ, Haynes TE, Hatakeyama K, Wu G (2004) Regulation of tetrahydrobiopterin synthesis and bioavailability in endothelial cells. *Cell Biochem Biophys* 41:415–433
- Szlas A, Kurek JM, Krejpcio Z (2022) The potential of L-arginine in prevention and treatment of disturbed carbohydrate and lipid metabolism—a review. *Nutrients* 14:961
- Tan B, Yin Y, Liu Z, Tang W, Xu H, Kong X, Xi L, Yao K, Gu W, Smith SB, Wu G (2011) Dietary L-arginine supplementation differentially regulates expression of lipid-metabolic genes in porcine adipose tissue and skeletal muscle. *J Nutr Biochem* 22:441–445
- Viollet B, Foretz M, Guigas B, Horman S, Dentin R, Bertrand L, Hue L, Andreelli F (2006) Activation of AMP-activated protein kinase in the liver: a new strategy for the management of metabolic hepatic disorders. *J Physiol* 574:41–53
- Wang YX, Watford M (2007) Glutamine, insulin and glucocorticoids regulate glutamine synthetase expression in C2C12 myotubes, Hep G2 hepatoma cells and 3T3 L1 adipocytes. *Biochim Biophys Acta* 1770:594–600
- Wang JJ, Chen LX, Li DF, Yin YL, Wang XQ, Li P, Dangott LJ, Hu WX, Wu G (2008) Intrauterine growth restriction affects the proteomes of the small intestine, liver and skeletal muscle in newborn pigs. *J Nutr* 138:60–66
- Williams G, Brown T, Becker L, Prager M, Giroir BP (1994) Cytokine-induced expression of nitric oxide synthase in C2C12 skeletal muscle myocytes. *Am J Physiol* 267:R1020–1025
- Wu G (2022) Amino acids: biochemistry and nutrition, 2nd edn. CRC Press, Boca Raton
- Wu G, Meininger CJ (2002) Regulation of nitric oxide synthesis by dietary factors. *Annu Rev Nutr* 22:61–86
- Wu G, Morris SM Jr (1998) Arginine metabolism: nitric oxide and beyond. *Biochem J* 336:1–17
- Wu G, Thompson JR (1990) The effect of glutamine on protein turnover in chick skeletal muscle in vitro. *Biochem J* 265:593–598

- Wu G, Knabe DA, Yan W, Flynn NE (1995) Glutamine and glucose metabolism in enterocytes of the neonatal pig. *Am J Physiol* 268:R334-342
- Wu G, Bazer FW, Tuo W, Flynn SP (1996) Unusual abundance of arginine and ornithine in porcine allantoic fluid. *Biol Reprod* 54:1261-1265
- Wu G, Pond WG, Ott T, Bazer FW (1998) Maternal dietary protein deficiency decreases amino acid concentrations in fetal plasma and allantoic fluid of pigs. *J Nutr* 128:894-902
- Wu G, Flynn NE, Flynn SP, Jolly CA, Davis PK (1999) Dietary protein or arginine deficiency impairs constitutive and inducible nitric oxide synthesis by young rats. *J Nutr* 129:1347-1354
- Wu G, Haynes TE, Li H, Yan W, Meininger CJ (2001) Glutamine metabolism to glucosamine is necessary for glutamine inhibition of endothelial nitric oxide synthesis. *Biochem J* 353:245-252
- Wu G, Knabe DA, Kim SW (2004a) Arginine nutrition in neonatal pigs. *J Nutr* 134:2783S-2790S

Publisher's Note Springer Nature remains neutral with regard to jurisdictional claims in published maps and institutional affiliations.

Springer Nature or its licensor holds exclusive rights to this article under a publishing agreement with the author(s) or other rightsholder(s); author self-archiving of the accepted manuscript version of this article is solely governed by the terms of such publishing agreement and applicable law.